Irreversible inhibition of hepatic fatty acid salt uptake by photoaffinity labeling with 11,11-azistearate

W. Schmider,* A. Fahr,† R. Voges,† W. Gerok,** and G. Kurz[1],*

Institut für Organische Chemie und Biochemie der Universität Freiburg,* D-79104 Freiburg, Germany; Sandoz Pharma Ltd.,† CH-4002 Basel, Switzerland; and Medizinische Universitätsklinik Freiburg,** D-79106 Freiburg, Germany

Abstract In order to have a model compound for detection of proteins involved in transport and metabolism of long-chain fatty acid salts by photoaffinity labeling 11,11-azistearate and 11,11-azi[G-³H]stearate (specific radioactivity 2.78 TBq/mmol) were synthesized. The suitability of 11,11-azi[G-³H]stearate for photoaffinity labeling was demonstrated by incorporation into BSA (bovine serum albumin) and H-FABP (hepatic fatty acid salt-binding protein) of rat liver. Repeated photoaffinity labeling resulted in a clear decrease of the binding capacities of both proteins. Labeling of protein mixtures with 11,11-azi[G-³H]stearate showed that binding proteins for long-chain fatty acid salts interact specifically with this probe. Photoaffinity labeling of isolated hepatocytes using 300 μM 11,11-azistearate in the presence of 100 μM BSA resulted in the irreversible inhibition of the uptake of stearate and its analogue 2,2,3,3,18,18,18-heptafluorostearate nearly to the same extent of about 30%. Irreversible inhibition of the uptake of long-chain fatty acid salts by photoaffinity labeling did not alter the mediated transport of cholyltaurine and has no effect on the uptake of 5β-cholestane-3α,7α,12α-triol, a compound that crosses the hepatocyte membrane by simple diffusion. ■ The irreversible inhibition of membrane transport by photoaffinity labeling demonstrates the existence of a specific transport system for the uptake of long-chain fatty acid salts into hepatocytes.—**Schmider, W., A. Fahr, R. Voges, W. Gerok, and G. Kurz.** Irreversible inhibition of hepatic fatty acid salt uptake by photoaffinity labeling with 11,11-azistearate. *J. Lipid Res.* 1996. **37:** 739–753.

Supplementary key words membrane transport • carrier • H-FABP • long-chain fatty acid salt • metabolically stable fatty acid salt

Membrane transport of salts of long-chain fatty acids is still a matter of controversy. On the one hand, membrane permeation of fatty acid salts is assumed to occur by simple diffusion (1–6) and on the other hand, a carrier-mediated process has been suggested (7–14). The assumption of simple diffusion is supported by the observation that weak carboxylic acids with pK_a values of about 5, such as fatty acids, pass through protein-free phospholipid bilayers, whereas sulfonic acids having pK_a values <2, like cholyltaurine, do not enter the inner leaflet (15). The assumption of mediated transport of long-chain fatty acid salts is justified by kinetic arguments such as Na^+ dependency, inhibition by alternative substrates, and a characteristic temperature dependency. Several proteins, identified by different methods, have been proposed so far as membrane transporters of fatty acid salts in mammalian tissues (16–21).

An interesting hypothesis assumes the existence of an albumin receptor, facilitating the dissociation of the fatty acid salt from the albumin–ligand complex prior to membrane transport (22, 23). However, proof of a direct involvement of BSA binding sites in the cell surface is still a matter of controversy (24–26).

The crucial point in kinetic studies of transport of long-chain fatty acid salts is their low solubility in aqueous solutions (27), limiting the concentration range necessary for determination of kinetic uptake mechanisms and of kinetic parameters. Therefore, it is the common practice to add albumin to solutions containing fatty acid salts. But, the addition of albumin leads to the controversy as to whether the uptake rate is a function of the concentration of unbound, of albumin-bound, or of the total concentration of fatty acid salt. An additional complication is caused by the fact that a small amount of the fatty acid salt (about 0.4%) exists in the protonated form at physiological pH values. Moreover, the extent of protonation of fatty acids incorpo-

---

rated into membranes is increased because their pK_a values are shifted from about 5 to about 8 (28, 29). The pK_a shift of fatty acids incorporated into lipid bilayers is affected by many factors and its influence on the rate of sinusoidal uptake of fatty acid salts is difficult to estimate. Thus, it is quite conceivable that the protonated part passes the plasma membrane by simple diffusion and the anionic form is taken up by a carrier-mediated process.

In order to overcome the problems of protonation and metabolism of natural fatty acid salts, an analogue of stearate and an appropriate derivative of it, amenable to photoactivation, were synthesized in which the hydrogen atoms at carbons 2, 3, and 18 were replaced by fluorine (30). As the substitution of hydrogen by fluorine leads to a derivative with comparable geometry, this exchange is regarded as an isogeometric transformation. This fluorinated fatty acid possesses a pK_a value of about 0.5 and the extent of its protonation may be neglected under physiological conditions. Moreover, this stearate analogue and its photolabile derivative are metabolically inert and allow, therefore, the study of transport and binding processes without the interference by metabolic reactions. However, conclusions drawn from results obtained with heptafluorostearate and its photolabile derivative are biologically valid only if the fluorinated compounds behave in transport as true analogues of the physiological fatty acid salt stearate. In order to exclude reservations against the application of the fluorinated fatty acid salts, a convenient synthesis of a photolabile derivative of nonfluorinated stearate was worked out. With the aid of this derivative there was demonstrated both the existence of a transport system for long-chain fatty acid salts in the plasma membrane of hepatocytes and the analogy of heptafluorostearate with stearate in hepatic membrane transport.

MATERIALS AND METHODS

Materials

Silica gel 60 (ICN Silica 32–63 μm, 60 Å) was purchased from ICN Biomedicals (Meckenheim, Germany). Silica gel plates (silica gel 60, 10 × 20 cm) for TLC were from E. Merck (Darmstadt, Germany). Palladium on charcoal (10% Pd) and stearic acid were obtained from Aldrich GmbH & Co. KG (Steinheim, Germany). ADIFAB was purchased from Molecular Probes Europe (Leiden, The Netherlands). BSA (bovine serum albumin, fraction V, essentially fatty acid-free), Coomassie Brilliant Blue R-250, Lipidex-1000, and cholyltaurine (Na+ salt) were from Sigma Chemie GmbH (Deisenhofen, Germany). Collagenase "Worthington" CLS II

with a specific activity of 125–150 U/mg protein was obtained from Biochrom KG (Berlin, Germany). Silicone oils AR20 and AR200 were purchased from Wacker Chemie (München, Germany). Trypan blue was from Serva (Heidelberg, Germany). Sodium heptafluorostearate, sodium 2, 2 ,3, 3, 18, 18, 18 - heptafluoro[G-3H]octadecanoate (2.63 TBq/mmol), 5β-cholestane- 3α,7α,12α-triol, 5β-[7β-3H]cholestane-3α, 7α,12α-triol (92.5 GBq/mmol), and cholyl[2'-3H(N)]taurine (0.75–1.5 TBq/mmol) were synthesized, and H-FABP was isolated as previously described (30–33). [1-14C]Stearic acid (2.15 GBq/mmol) and [G-3H]inulin (88.8 GBq/mmol) were purchased from Amersham Buchler (Braunschweig, Germany). Tritium gas (carrier-free, 96.2 GBq/ml) was purchased from RC TRITEC AG (Teufen, Switzerland). All other chemicals were of highest quality available from commercial sources.

Animals

Male Wistar rats (Tierzuchtanstalt Jautz, Hannover, Germany) weighing 200–250 g were used. The animals had free access to food (standard rat diet Altromin 300 R, Altromin GmbH, Lage, Germany) and tap water, and were housed in a constant temperature environment with natural day–night rhythm.

Protein determination and detection of radioactivity

Protein concentration, radioactivity in solutions, and radioactivity in polyacrylamide gels were determined as described (34–36). The amount of H-FABP in hepatocytes was estimated after SDS-PAGE of total cell protein. Subsequent to staining with Coomassie Brilliant Blue R-250, the relative absorption at 633 nm of the protein band with the apparent molecular weight of 14,000 was determined using a laser densitometer Ultrascan XL (Pharmacia LKB, Freiburg, Germany). For quantification the relative absorption of this band was compared to the values obtained with known amounts of isolated H-FABP subjected to SDS-PAGE on the same gel plate.

Isolation and characterization of hepatocytes

Isolation and characterization of hepatocytes from rats was carried out as described (35) using a slightly modified medium to improve its buffer capacity. The modified standard medium containing 118 mM NaCl, 4.74 mM KCl, 1.2 mM $MgCl_2$, 0.59 mM KH_2PO_4, 0.59 mM Na_2HPO_4, 14 mM $NaHCO_3$, 10 mM HEPES, 5.5 mM D-glucose, and 1.25 mM $CaCl_2$ (absent in the Ca^{2+}-free medium), was saturated with carbogen (95% O_2/5% CO_2) and adjusted to pH 7.4 with 5 M NaOH.

Preparation of protein-containing solutions of long-chain fatty acid salts

Whereas protein-containing solutions of heptafluorostearate can be directly prepared by addition of ethanolic solutions of the compound to the protein solution in standard medium, the preparation of solutions of stearate or 11,11-azistearate requires a different procedure to avoid precipitation of the long-chain fatty acid salts.

Protein was first dissolved in 96% of the required final volume of a medium consisting of 123 mM NaCl, 4.94 mM KCl, 0.61 mM KH$_2$PO$_4$, 0.61 mM Na$_2$HPO$_4$, 14.6 mM NaHCO$_3$, 10.4 mM HEPES, 5.7 mM D-glucose, saturated with carbogen (95% O$_2$/5% CO$_2$) and adjusted to pH 7.4 with 5 M NaOH. After addition of the ethanolic solution of stearate or 11,11-azistearate (<1% of the final volume), 4% of the required final volume of an aqueous solution of 30 mM MgCl$_2$ and 31.25 mM CaCl$_2$ or of pure water for experiments performed in the absence of bivalent cations were added.

Photolyses

Photolyses and photoaffinity labeling experiments were carried out at a wavelength of 350 nm and 30°C if not stated otherwise, using a Rayonet RPR 100 reactor (The Southern Ultraviolet Company, Hamden, CT) equipped with 16 RPR 3500 Å lamps (32). Ultraviolet absorption spectra were measured with a Perkin-Elmer UV/VIS-Spectrometer Lambda 5 (Perkin-Elmer, Überlingen, Germany). As 11,11-azistearate is light- and temperature-sensitive, the compound was monitored by UV-spectroscopy every time before use.

Photoaffinity labeling of isolated proteins

Photoaffinity labeling of isolated proteins and of mixtures of isolated proteins was carried out after preincubation with the photolabile derivative in the dark for 10 min. Photoaffinity labeling of pure BSA or H-FABP was performed in 300 µl of standard medium containing 1 µM of the respective protein and 30 nM (25 kBq) 11,11-azi[G-^{3}H] stearate for diffferent lengths of time. Mixtures of several purified proteins (100 µg of each) and 90 nM (100 kBq) 11,11-azi[G-^{3}H]stearate in 400 µl standard medium were irradiated for 10 min. Subsequent to photoaffinity labeling the proteins were precipitated by addition of methanol and chloroform and submitted to SDS-PAGE (36).

Photoaffinity labeling in the deep-frozen state was followed after shock-freezing the corresponding solutions in liquid nitrogen (36). Prior to shock-freezing, solutions of 1 µM BSA or H-FABP with 30 nM (50 kBq) 11,11-azi[G-^{3}H]stearate in 600 µl standard medium in the presence of different concentrations of stearate or heptafluorostearate were incubated for 10 min in the dark. After incubation the samples were shock-frozen by transfer into quartz test tubes precooled in liquid nitrogen. The frozen samples were irradiated for 15 min in the photoreactor. To prevent thawing of the samples they were cooled in liquid nitrogen every 30 sec during the irradiation procedure. Subsequent to photolysis the samples were thawed and the proteins were precipitated and subjected to SDS-PAGE (36).

Photoaffinity labeling of isolated hepatocytes

Photoaffinity labeling of isolated hepatocytes prior to uptake studies was performed with 5 ml of a hepatocyte suspension (5–6 × 10^6 cells/ml corresponding to 10–12 mg protein/ml) in standard medium containing 100 µM BSA and 300 µM of 11,11-azistearate for 10 min without preincubation. Subsequent to photoaffinity labeling the hepatocytes were separated from the incubation medium by centrifugation at 35 g for 2 min, and resuspended in 30 ml of a solution of 100 µM BSA in standard medium. The suspension was incubated at 37°C for 10 min and centrifuged again at 35 g for 2 min. After repeating this procedure four times, the procedure was carried out twice using 30 ml of standard medium containing no BSA. After a final centrifugation at 35 g for 2 min, the cells were suspended in standard medium at a concentration of 2–2.5 × 10^6 cells/ml corresponding to 4–5 mg protein/ml and were allowed to recover at 37°C for 30 min. For a control, the complete experimental procedure was performed under identical conditions with cell suspensions in presence of stearate or 11,11-azistearate, omitting irradiation in the latter case. Cell viability was determined as described (35).

In order to estimate the extent of labeling of extracellular BSA and cellular binding proteins under the conditions applied, a known amount of 11,11-azi[G-^{3}H]stearate was added to the incubation mixture. Subsequent to photoaffinity labeling, incorporation of radioactivity into polypeptides was determined after SDS-PAGE.

Determination of binding capacity

Binding of stearate or heptafluorostearate to BSA and H-FABP prior to and after photoaffinity labeling with 11,11-azistearate was studied as described (37) using the fluorescent probe ADIFAB as an indicator for free fatty acid salts. The concentration of free fatty acid salts was estimated with the aid of a Luminescence Spectrometer LS 50 B (Perkin-Elmer) from the ratio of the fluorescence intensities at 505 nm and 432 nm with slit widths of 10 nm using excitation at 390 nm and a slit width of 5 nm. The protein concentrations used were 0.2 µM for ADIFABP and BSA and 0.4 µM for H-FABP. Stock solutions of [1-^{14}C]stearate or [^{3}H]heptafluorostearate of defined specific radioactivity in 5 mM NaOH were

added to the protein mixture, and the total fatty acid salt concentration in the assay was estimated from the radioactivity in an aliquot.

Uptake studies

Uptake of compounds into freshly isolated hepatocytes was determined using the centrifugal filtration technique through a silicone oil layer using the conditions described previously (35). Uptake measurements were routinely performed from 10 sec up to 60 sec in 10-sec intervals. Initial rates of uptake were calculated by linear regression analysis from the linear portion of the time-dependent uptake curves. The slope of a straight line through these data points was considered as the initial rate. The intercept of the determined straight line with the ordinate corresponded with the radioactivity in the volume adherent to the cells, as measured with [G-^{3}H]inulin.

HPLC

HPLC was carried out on a reversed-phase column with an LKB 2150 liquid chromatograph (Pharmacia LKB, Freiburg, Germany) equipped with a Rheodyne injector 7150 (Rheodyne Inc., Cotati, CA), a UV wavelength detector (Rapid Spectral Detector, Pharmacia LKB, Freiburg, Germany) and a flow-through monitor Ramona 90 (Raytest, Straubenhardt, Germany). Nonradioactive azi compounds were detected at 350 nm. A semi-preparative Zorbax ODS column RP18 (250 × 9.6 mm I.D., 5-μm particles, DuPont Instruments, Bad Nauheim, Germany) and an analytical μBondapak column RP18 (220 × 4.6 mm I.D., 5-μm particles, Waters GmbH, Eschborn, Germany) were used with solvent system A, acetonitrile–water 95:5 (v/v) or solvent system B, acetonitrile–water–trifluoroacetic acid 80:20:0.1 (v/v/v). The flow rate was 2 ml/min at 25°C in both cases.

Analysis of organic compounds

Melting points were determined with a Büchi hot-stage apparatus (Büchi, Flawil, Switzerland) and are uncorrected. ^{1}H-NMR spectra were measured on a Bruker-250-MHz spectrometer (Bruker GmbH, Karlsruhe, Germany). Values are given in parts per million relative to tetramethylsilane as internal standard. Mass spectra were determined with a Finnigan 44S mass spectrometer connected with a data unit SS 2000 (Finnigan, Sunnyvale, CA). The compounds were ionized by EI (electron impact ionization) with an electron energy of 70 eV, and by DCI (direct chemical ionization) with an electron energy of 170 eV using ammonia or isobutane as reactant gas at a pressure of 30 Pa, and in both cases positive ions were recorded (38). Elemental analyses were performed using a Perkin-Elmer 240 ana-

lyzer (Perkin-Elmer, Friedrichshafen, Germany). After TLC the organic compounds were visualized by spraying the dried plates with 0.1 N KMnO$_4$ or with 1% (w/v) vanillin in H$_2$SO$_4$ and subsequent heating at 100°C for 30 sec.

Syntheses

Preparative separations of nonradioactive compounds were performed either on 20 × 5 cm columns of silica gel 60 (32–63 μm) using flash chromatography (39) or on 50 × 5 cm columns of the same gel at hydrostatic pressure. Preparative separations of radioactive compounds were performed on a 20 × 2 cm column of the same silica gel using flash chromatography. Solvent systems for chromatographic separations were: solvent system 1, cyclohexane–ethyl acetate 30:1 (v/v); solvent system 2, cyclohexane–ethyl acetate 15:1 (v/v); solvent system 3, cyclohexane–ethyl acetate 11:1 (v/v); solvent system 4, cyclohexane–ethyl acetate 5:1 (v/v); solvent system 5, cyclohexane–ethyl acetate 2:1 (v/v); solvent system 6, cyclohexane–ethyl acetate 1:1 (v/v); solvent system 7, ethyl acetate–cyclohexane–acetic acid 100:40:1 (v/v/v); solvent system 8, ethyl acetate–cyclohexane–acetic acid 1:30:3 (v/v/v).

tert-Butyl 10-undecenoate (**II**) (**Fig. 1**). Starting with 10-undecenoyl chloride (**I**) *tert*-butyl 10-undecenoate was prepared principally as described (40). A solution of 28 ml (0.3 mol) of freshly distilled *tert*-butyl alcohol and 42 ml (0.3 mol) of freshly distilled N,N-dimethylaniline in 40 ml of dry ether was heated to refluxing. Under an atmosphere of nitrogen, 43 ml (0.2 mol) of 10-undecenoyl chloride was added at such a rate that moderate refluxing continued after the heating had been removed. Then, the reaction mixture was refluxed for 1 h. After cooling to room temperature 40 ml of water was added, and stirring was continued until all solid material was dissolved. The ether layer was separated and extracted several times with 2 M hydrochloric acid until the extract no longer became cloudy when made alkaline. After a final washing with 20 ml of saturated sodium bicarbonate, the ether phase was dried over Na$_2$SO$_4$. The solution was filtered, and the solvent was removed under reduced pressure. The residue was purified by distillation under reduced pressure yielding 43 g (0.18 mol, 90% yield) of pure product. BP, 85°C (50 Pa); TLC: R_f = 0.47 (solvent system 2), 0.61 (solvent system 4); ^{1}H-NMR (CDCl$_3$): δ = 1.30 (m,CH$_2$-4/5/6/7/8), 1.45 (s,OC(CH$_3$)$_3$), 1.55 (m,CH$_2$-3), 2.05 (m,CH$_2$-9), 2.21 (t,J =7 Hz,CH$_2$-2), 4.85 (d,J = 8 Hz, CH-11,trans), 4.95 (d,J = 15 Hz, CH-11, *cis*), 5.80 (m, CH-10);mass spectrum (EI): *m/z* = 184, M–C$_4$H$_8$; mass spectrum (DCI, isobutane): *m/z* = 241, (M+H)$^+$; anal. calcd. for C$_{15}$H$_{28}$O$_2$ (240.39): C, 74.95, H, 11.74; found: C, 75.57, H, 11.81.
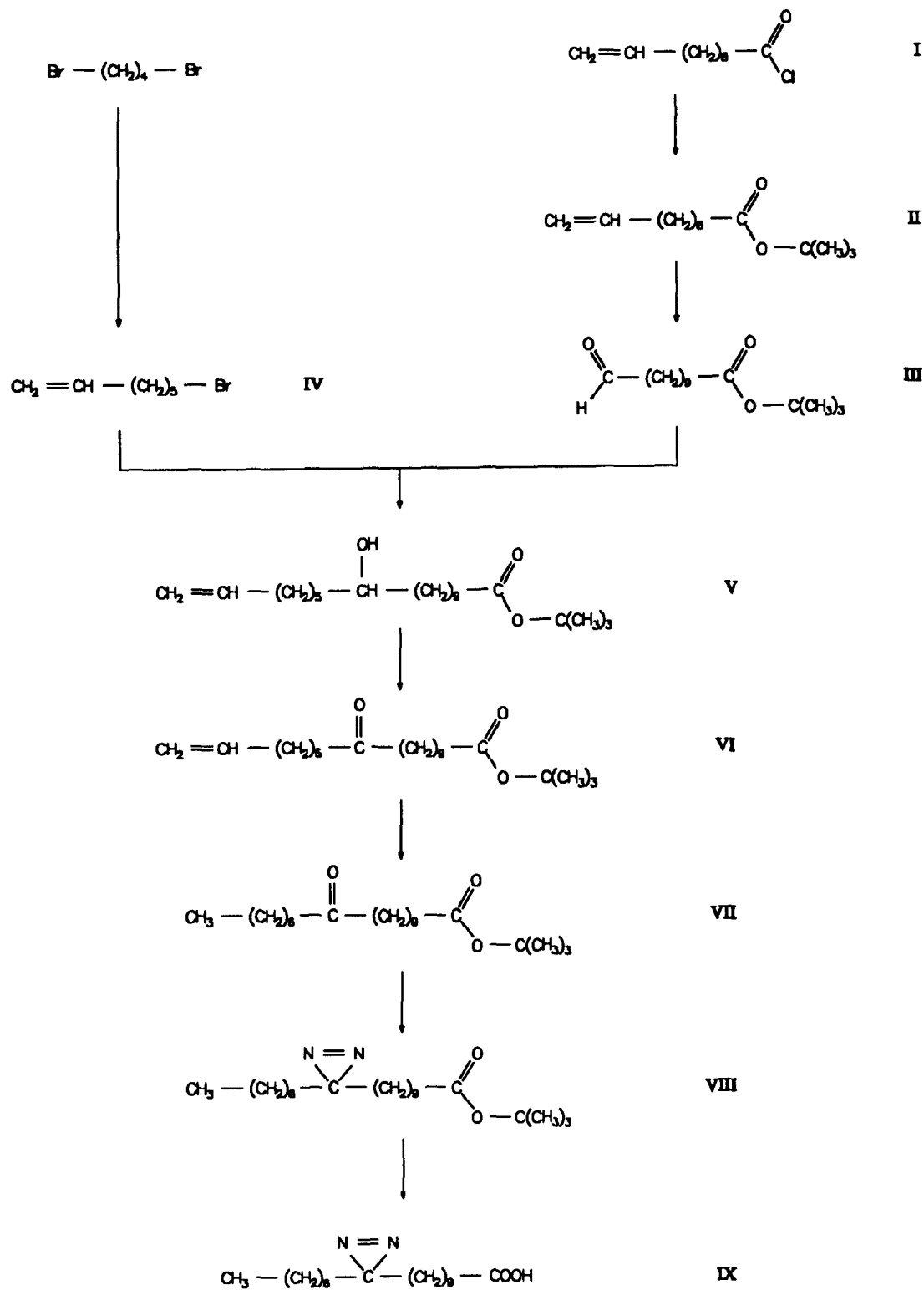
Fig. 1. Reaction scheme for the synthesis of azi derivatives of long-chain fatty acids.

tert-Butyl 11-oxoundecanoate (**III**) (Fig. 1). The tert-butyl 11-oxoundecanoate was synthesized principally as described (41, 42). In an oven-dried, nitrogen-flushed flask, 2.04 ml (20 mmol) of borane–methyl sulfide (9.8 M in tetrahydrofurane) and 20 ml of dry methylene chloride were placed. To this solution 14.4 g (60 mmol) of *tert*-butyl 10-undecenoate were added dropwise at room temperature with vigorous stirring. After stirring the reaction mixture for an additional hour, the solvent and methyl sulfide were removed under reduced pressure. The resulting crude alkylborane was added dropwise at room temperature to a well-stirred suspension of 38.3 g (180 mmol) of pyridinium chlorochromate in 150 ml of dry methylene chloride. After stirring for 15 min, the mixture was diluted with 200 ml of dry ether and filtered through a 5 × 40 cm glass column containing 100 g of silica gel. Subsequently, the residue on the silica gel was treated 3 times with 50-ml portions of dry ether, the organic phases were combined, and the solvent was removed under reduced pressure. The crude product was purified by chromatography under hydrostatic pressure using solvent system 3. The yield of pure product was 7.7 g (10 mmol, 50% yield). TLC: $R_f \approx 0.36$ (solvent system 4), 0.55 (solvent system 5); ^{1}H-NMR (CDCl$_3$): δ = 1.30 (m,CH$_2$-4/5/6/7/8), 1.45 (s,OC(CH$_3$)$_3$), 1.60 (m,CH$_2$-3/9), 2.21 (t,J = 7 Hz,CH$_2$-2), 2.40 (m,CH$_2$-10), 9.8 (t,J = 1.6 Hz,CH-11); mass spectrum (EI): m/z = 199, M–C(CH$_3$)$_3$; mass spectrum (DCI, ammonia): m/z = 274, (M+NH$_4$)$^+$; 256, M+NH$_4$–H$_2$O; anal. calcd. for C$_{15}$H$_{28}$O$_3$ (256.39): C, 70.27, H, 11.01; found: C, 70.48, H, 11.03.

tert-Butyl 11-hydroxy-17-octadecenoate (**V**) (Fig. 1). The *tert*-butyl 11-hydroxy-17-octadecenoate was synthesized principally as described (43). A sample of 0.8 g (33 mmol) of magnesium turnings was suspended in 15 ml of dry ether, and the suspension was allowed to react with a few drops of a solution of 5.3 g (30 mmol) of 7-bromo-1-heptene (**IV**) (Fig. 1) in 15 ml of dry ether. The bromo compound was synthesized as described (44). When the violent reaction had started, the 7-bromo-1-heptene solution was added at such a rate that the mixture boiled gently. After refluxing for 1 h, the mixture was cooled to room temperature and filtered through a D1-frit. Under an atmosphere of nitrogen the filtrate was dropped slowly to a vigorously stirred solution of 7 g (27 mmol) of *tert*-butyl 11-oxoundecanoate in 30 ml of dry ether cooled to -30°C. As the precipitate formed during the reaction tended to stop the stirring bar, a further 20 ml of dry ether was added to the reaction mixture as soon as half of the filtrate had been added. After the addition of the metallorganic compound had been completed, the mixture was stirred at room temperature for 15 min. Then, the reaction mixture was decomposed with ice water and neutralized with 2 M hydrochloric acid. After separation of the

organic phase, the aqueous phase was extracted 3 times with 50 ml of ether. The combined organic phases were dried over Na$_2$SO$_4$, and after filtration the solvent was removed under reduced pressure. The crude product was purified by chromatography under hydrostatic pressure using solvent system 3. The yield of pure product was 4.3 g (0.12 mmol, 45% yield). MP, 27°C; TLC: R_f = 0.32 (solvent system 4), 0.61 (solvent system 6); ^{1}H-NMR (CDCl$_3$): δ = 1.30 (m,CH$_2$-4/5/6/7/8/9/13/14/15), 1.45 (m,OC(CH$_3$)$_3$/CH$_2$-10/12), 1.55 (m,CH$_2$-3), 2.05 (m,CH$_2$-16), 2.20 (t,J = 7 Hz,CH$_2$-2), 3.60 (m,CH-11), 4.85 (d,J = 8 Hz,CH-18,*trans*), 4.95 (d,J = 15 Hz,CH-18,*cis*), 5.8 (m,CH-17); mass spectrum (EI): m/z = 201, M–(CH$_2$C(CH$_3$)$_2$+C$_7$H$_{13}$); mass spectrum (DCI, isobutane): m/z = 355, (M+H)$^+$; 299, M+H–CH$_2$C(CH$_3$)$_2$; anal. calcd. for C$_{22}$H$_{42}$O$_3$ (354.56): C, 74.52, H, 11.94; found: C, 74.40, H, 11.85.

tert-Butyl 11-oxo-17-octadecenoate (**VI**) (Fig. 1). The *tert*-butyl 11-oxo-17-octadecenoate was synthesized principally as described (45). A solution of 2.67 g (27 mmol) of chromic acid in 2.3 ml of concentrated sulfuric acid and 4 ml of water was adjusted to a final volume of 10 ml. A sample of 4.6 g (13 mmol) of *tert*-butyl 11-hydroxy-17-octadecenoate was dissolved in 35 ml of acetone. Under cooling in an ice bath the chromic acid solution (about 3 ml) was added dropwise until a persistent orange coloration indicated the end of the reaction. After dilution with 200 ml of ice water, the mixture was extracted 3 times with 100 ml of ether. The combined ether phases were dried over Na$_2$SO$_4$, the solution was filtered, and the solvent was removed under reduced pressure. The crude product was purified by flash chromatography using solvent system 1. The yield of pure product was 4.1 g (90% yield). MP, 25°C; TLC: R_f = 0.29 (solvent system 2), 0.52 (solvent system 4); ^{1}H-NMR (CDCl$_3$): δ = 1.30 (m,CH$_2$-4/5/6/7/8/14/15), 1.45 (m,OC(CH$_3$)$_3$), 1.55 (m,CH$_2$-3/9/13), 2.05 (m,CH$_2$-16), 2.20 (t,CH$_2$-2), 2.40 (t,J = 7 Hz,CH$_2$-10/12), 4.85 (d,J = 8 Hz,CH-18,*trans*), 4.95 (d,J = 15 Hz,CH-18,*cis*), 5.8 (m,CH-17); mass spectrum (EI): m/z = 296, M–CH$_2$C(CH$_3$)$_2$; 214, M–(CH$_2$C(CH$_3$)$_2$+C$_6$H$_{10}$); 199, M–(CH$_2$C(CH$_3$)$_2$+C$_7$H$_{13}$); mass spectrum (DCI, ammonia): m/z = 370, (M+NH$_4$)$^+$; anal. calcd. for C$_{22}$H$_{40}$O$_3$ (352.54): C, 74.95, H, 11.44; found: C, 75.24, H, 11.36.853O

tert-Butyl 11-oxooctadecanoate (**VII**) (Fig. 1). The *tert*-butyl 11-oxooctadecanoate was synthesized by catalytic reduction of 1.4 g (4 mmol) of *tert*-butyl 11-oxo-17-octadecenoate following the procedure described (30). Flash chromatography of the crude product in solvent system 1 yielded 1.3 g (95% yield) of the pure product. MP, 38°C; TLC: R_f = 0.30 (solvent system 2), 0.53 (solvent system 4); ^{1}H-NMR (CDCl$_3$): δ = 0.88 (t,J = 7 Hz,CH$_3$-18), 1.30 (m,CH$_2$-4/5/6/7/8/14/15/16/17),

1.45 (m,OC(CH$_3$)$_3$), 1.55 (m,CH$_2$–3/9/13), 2.20 (t,J = 7 Hz,CH$_2$–2), 2.40 (t,J = 7 Hz,CH$_2$–10/12); mass spectrum (EI): m/z = 298, M–CH$_2$C(CH$_3$)$_2$; 214, M–(CH$_2$C(CH$_3$)$_2$+C$_6$H$_{12}$); 199, M–(CH$_2$C(CH$_3$)$_2$+C$_7$H$_{15}$); mass spectrum (DCI, isobutane): m/z = 355, (M+H)$^+$; 299, M+H–CH$_2$C(CH$_3$)$_2$; anal. calcd. for C$_{22}$H$_{42}$O$_3$ (354.56): C, 74.52, H, 11.94; found: C, 74.50, H, 12.01.

tert-Butyl 11,11-azioctadecanoate (**VIII**) (Fig. 1). The *tert*-butyl 11,11-azioctadecanoate was synthesized principally as described (46, 47). A sample of 1 g (2.8 mmol) of *tert*-butyl 11-oxooctadecanoate was dissolved in 250 ml of a 1:1 mixture (v/v) of dry methanol and dry ethanol. Dry ammonia was bubbled through this solution at 0°C for 2 h. Then, a solution of 1.5 g (13 mmol) of hydroxylamine-O-sulfonic acid in 20 ml of dry methanol was added in small portions at 0°C. The suspension was stirred at room temperature overnight and filtered through a D4-frit. After addition of 1.5 ml of freshly distilled triethylamine, the filtrate was evaporated. The residue was dissolved in 40 ml of methanol, and 2.5 ml of triethylamine were added. The following procedures were performed in the dark. A solution of 0.7 g (2.8 mmol) of iodine in 5 ml of methanol was added at room temperature within 20 min. A persistent orange-red coloration indicated the end of the reaction. The mixture was evaporated under reduced pressure, and the crude product was purified by flash chromatography using solvent system 1. Fractions containing the reaction product (R_f = 0.48 in solvent system 2) were collected, and the solvent was removed under reduced pressure. The residue was purified by HPLC with a semi-preparative column (250 × 9.6 mm I.D.) using solvent system A. The yield of pure product was 0.2 g (20% yield). The product was stored in the dark at -80°C. MP, 31°C; TLC: R_f = 0.48 (solvent system 2), 0.64 (solvent system 4); HPLC: t_R = 41.7 min (semi-preparative column and solvent system A); ^{1}H-NMR (CDCl$_3$): δ = 0.88 (t,J = 7 Hz,CH$_3$–18), 1.06 (m,CH$_2$–10/12), 1.30 (m,CH$_2$–4/5/6/7/8/9/13/14/15/16/17), 1.45 (m,OC(CH$_3$)$_3$), 1.55 (m,CH$_2$–3), 2.20 (t,J = 7 Hz,CH$_2$–2); mass spectrum (DCI, ammonia): m/z = 384, (M+NH$_4$)$^+$; 367, (M+H)$^+$; 328, M+NH$_4$–CH$_2$C(CH$_3$)$_2$; anal. calcd. for C$_{22}$H$_{42}$N$_2$O$_2$ (366.58): C, 72.08, H, 11.55, N, 7.64; found: C, 71.80, H, 11.44, N, 7.71.

11,11-Azioctadecanoic acid (**IX**) (Fig. 1). The 11,11-azioctadecanoic acid was synthesized principally as described (48). A sample of 200 mg (0.55 mmol) of *tert*-butyl 11,11-azioctadecanoate was dissolved in 2.5 ml of trifluoroacetic acid and stirred in the dark at room temperature for 5 min. The mixture was evaporated under reduced pressure. The crude product was purified by flash chromatography using solvent system 8 and, finally, by HPLC with a semi-preparative column (250 × 9.6 mm I.D.) and solvent system B. The yield of

pure product was 150 mg (0.5 mmol, 90% yield). The product was stored in the dark at -80°C. MP, 52°C; TLC: R_f = 0.64 (solvent system 7), 0.30 (solvent system 8); HPLC: t_R = 14.0 min (semi-preparative column and solvent system B); ^{1}H-NMR (CDCl$_3$): δ = 0.88 (t,J = 7 Hz,CH$_3$–18), 1.06 (m,CH$_2$–10/12), 1.30 (m,CH$_2$–4/5/6/7/8/9/13/14/15/16/17), 1.61 (m,CH$_2$–3), 2.35 (t,J = 7 Hz,CH$_2$–2); mass spectrum (DCI, ammonia): m/z = 328, (M+NH$_4$)$^+$; 300, M+NH$_4$–N$_2$; anal. calcd. for C$_{18}$H$_{34}$N$_2$O$_2$ (310.47): C, 69.63, H, 11.04, N, 9.02; found: C, 69.50, H, 11.08, N, 9.11.

Syntheses of radioactively labeled fatty acid derivatives

tert-Butyl 11-oxo[G-^{3}H]octadecanoate (**VII**) (Fig. 1). The tritiation of *tert*-butyl 11-oxooctadecenoate was performed exactly as described (30) by catalytic reduction of 7.4 mg (21 μmol) of *tert*-butyl 11-oxooctadecenoate with 185 GBq tritium gas. The reaction product was purified by flash chromatography using solvent system 1 to give 7 mg (20 μmol, 95%) of the product. It was shown by TLC/radio–TLC (TLC-Analyzer LB 2820, Berthold, Wildbad, Germany) to be chemically and radiochemically pure. In order to minimize radiolytic decomposition, the product was dissolved in 50 ml of ethyl acetate and stored at -80°C. The specific activity of 7.9 GBq/mg or 2.78 TBq/mmol, respectively, corresponded to a radiochemical yield of 30%.

tert-Butyl 11,11-azi[G-^{3}H]octadecanoate (**VIII**) (Fig. 1). A sample of 11 GBq (4.2 μmol) *tert*-butyl 11-oxo[G-^{3}H]octadecanoate was dissolved in 500 μl of a 1:1 mixture (v/v) of dry methanol and dry ethanol. Dry ammonia was bubbled through the solution at 0°C for 3 h. Under stirring, a solution of 15 mg (133 μmol) of hydroxylamine-O-sulfonic acid in 120 μl of dry methanol and 80 μl of dry ethanol was added slowly. The resulting suspension was stirred at room temperature overnight. The mixture was filtered through a D4-frit, treated with 50 μl of triethylamine, and evaporated. The resulting residue was dissolved in a mixture of 600 μl of methanol and 40 μl of triethanolamine. All further procedures were performed in the dark. After the addition of an iodine crystal, the mixture was stirred at room temperature for 2 h. The reaction mixture was evaporated, and the residue was treated several times with portions of 500 μl of ether. The combined ether phases were concentrated to 100 μl and subjected to flash chromatography using solvent system 1. The fractions containing reaction product (R_f = 0.48 in solvent system 2) were collected, and the solvent was removed under reduced pressure. The crude product was purified by HPLC using an analytical column (220 × 4.6 mm I.D.) with solvent system A. The radiochemical yield of pure product was 1.9 GBq (17%) with the unchanged specific

activity of 2.78 TBq/mmol. The product was dissolved in 50 ml of ether and stored in the dark at -80°C.; HPLC: t_R = 8.6 min (analytical column with solvent system A).

11,11-Azi[G-³H]octadecanoic acid (**IX**) (Fig. 1). A sample of 1 GBq (0.36 μmol) *tert*-butyl 11,11-azi[G-³H]octadecanoate was dissolved in 1 ml of trifluoroacetic acid and stirred at room temperature in the dark for 5 min. The solvent was removed under reduced pressure, the crude product was purified by flash chromatography in solvent system 8, followed by HPLC using an analytical column (220 × 4.6 mm I.D.) and solvent system B. The yield of radiochemically pure product was 0.95 GBq (95%) with specific activity of 2.78 TBq/mmol. The radioactive compound was dissolved in 50 ml of ether and stored in the dark at -80°C. HPLC: t_R = 14.0 min (analytical column with solvent system B).

RESULTS AND DISCUSSION

Syntheses

A photolabile derivative is desired for the study of transport and metabolism of long-chain fatty acid salts and their involvement in signalling processes. The detection of specific transport systems, otherwise difficult to trace, and the identification of polypeptides involved in metabolic and regulatory processes are facilitated by photoaffinity labeling studies with suitable photolabile derivatives. The syntheses of heptafluorostearate and 11,11-azi-2,2,3,3,18,18,18-heptafluorooctadecanoate (30), as derivatives of stearate, were a step forward in the identification of polypeptides interacting with long-chain fatty acid salts (33, 49). But, due to the low pK_a value of 0.5 of the corresponding acids, these metabolically stable fluorinated derivatives are only applicable to the identification of polypeptides interacting with salts of free fatty acids and do not allow the synthesis of the CoA-thioesters needed for metabolic investigations. In order to extend photoaffinity labeling studies to metabolic processes of long-chain fatty acids, the synthesis of 11,11-azistearate was worked out. Furthermore, this compound was used for the final proof, otherwise difficult to furnish, that heptafluorostearate is a true competing substrate for membrane transport of stearate.

Because of its small spatial requirement, the azi group, whose favorable properties have been repeatedly shown (30–33), was selected for the synthesis of a photolabile analogue of the desired long-chain fatty acid salt. On account of the specificity of biological processes for a given range of fatty acid chain length, a synthesis was conceived that allowed both the variation of chain length and the introduction of the azi group in variable positions. The key step in the synthesis is the Grignard

reaction between the corresponding ω-oxo fatty acid ester and the respective alkenyl or alkyl magnesium halide. The resulting hydroxy compound can easily be transformed into the diazirine derivative (30–33).

For reasons of comparison, in the actual described synthesis the photolabile group was introduced in position 11 of stearate (**IX**) (Fig. 1) analogous to 11,11-azi-2,2,3,3,18,18,18-heptafluorooctadecanoate. The use of the *tert*-butyl group as a protecting group for the carboxyl function proved to be favorable because of its selective removability under the mild conditions required by the limited stability of the azi group. The requisite ω-oxo fatty acid ester (**III**) was obtained by hydroboration of the *tert*-butyl 10-undecenoate (**II**) with borane–methyl sulfide followed by oxidation of the intermediate alkyl borane with pyridinium chlorochromate in methylene chloride in a one-flask procedure. The following Grignard reaction with 6-heptenylmagnesium bromide led to *tert*-butyl 11-hydroxy-17-octadecenoate (**V**) bearing the hydroxy group at the selected position. After oxidation of the hydroxy compound (**V**) to the corresponding oxo derivative (**VI**) the terminal double bond was used for the introduction of the radioactive label by catalytic tritiation using carrier-free tritium gas in a 3 molar excess. The reaction proceeded even under a reduced pressure of about 40 kPa without any problems. The determined specific activity of 2.78 TBq/mmol corresponds to 2.6 tritium atoms/molecule. The incorporation of more than two theoretically expected tritium atoms originates from simultaneous H/T-exchange processes, a phenomenon that has also been observed in the catalytic tritiation of other unsaturated compounds (30, 50). In most syntheses of diazirine compounds, the final conversion of the oxo group into the corresponding azi group results in relative low yields. Actually, the circumstances were additionally complicated because a convenient solvent for *tert*-butyl 11-oxooctadecanoate (**VII**) and ammonia at the requisite low temperature was difficult to find. A 1:1 mixture (v/v) of methanol and ethanol finally proved to be the best compromise furnishing yields of about 20%. The protecting *tert*-butyl group was removed in the last step in trifluoroacetic acid at room temperature within 5 min to give the desired 11,11-azistearic acid (**IX**) in nearly quantitative yields.

Photolysis and conditions of photoaffinity labeling

The UV spectrum of 11,11-azistearic acid shows the two characteristic maxima for diazirine functions at 350 nm and 366 nm of which the latter is less pronounced (**Fig. 2A**). The extinction coefficient of 11,11-azistearic acid at 350 nm was determined to be ε = 86 $M^{-1}cm^{-1}$. Accordingly, photolyses and photoaffinity labeling experiments were performed with light having a wave-
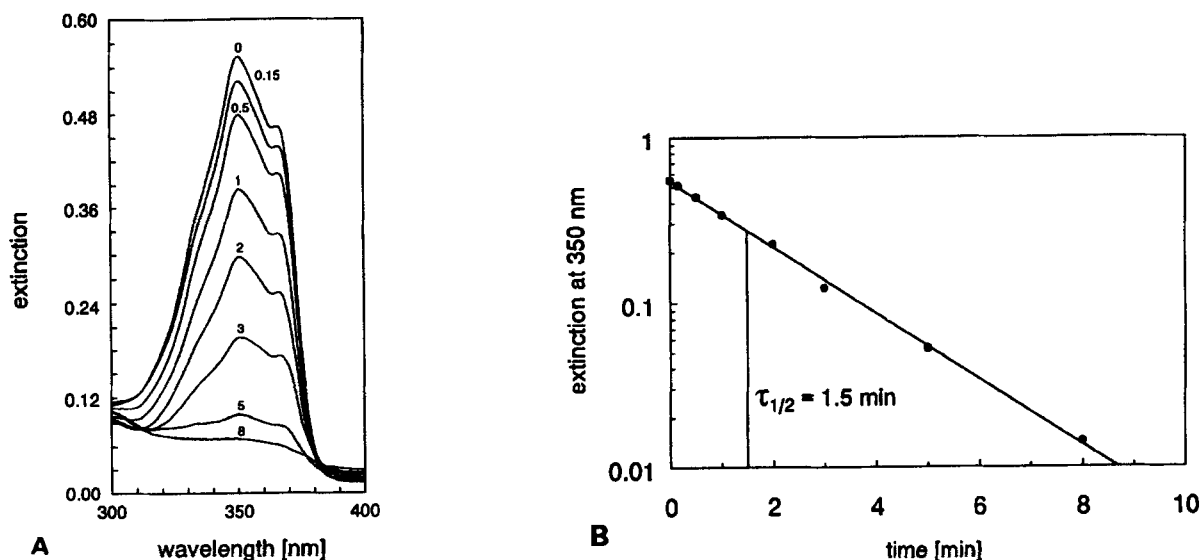
Fig. 2. Photolysis of 11,11-azistearic acid monitored by UV spectroscopy. A 6.4 mM solution of 11,11-azistearic acid in chloroform was photolyzed in a Rayonet RPR-100 photochemical reactor equipped with 16 RPR-3500 Å lamps for 0, 0.15, 0.5, 1, 2, 3, 5, and 8 min at 30°C. A: Recording of the UV spectra after the indicated times of irradiation. B: Logarithmic graph of the extinction at 350 nm after the different times of photolysis. The extinctions were corrected for the absorption at infinite irradiation time.

length of 350 nm. In order to evaluate the irradiation time necessary for photoaffinity labeling of biological material, the time dependency of photolysis of 11,11-azistearic acid in chloroform was examined (Fig. 2A). Under the experimental conditions used, photolysis followed first order kinetics with a half-life of 1.5 min (Fig. 2B).

In order to determine the conditions for photoaffinity labeling of fatty acid salt-binding proteins using 11,11-azistearate, photolysis of 11,11-azi[G-^{3}H]stearate was performed in the presence of BSA and H-FABP, respectively. As expected, photolysis of 30 nM (25 kBq) 11,11-[G-^{3}H]azistearate in the presence of 1 μM BSA or H-FABP resulted in a clear labeling of both proteins (**Fig. 3**). Incorporation of radioactivity increased with irradiation time during the first 5 min, as shown after SDS-PAGE for BSA (**Fig. 4**). Without irradiation, practically no covalently bound radioactivity was detected in the
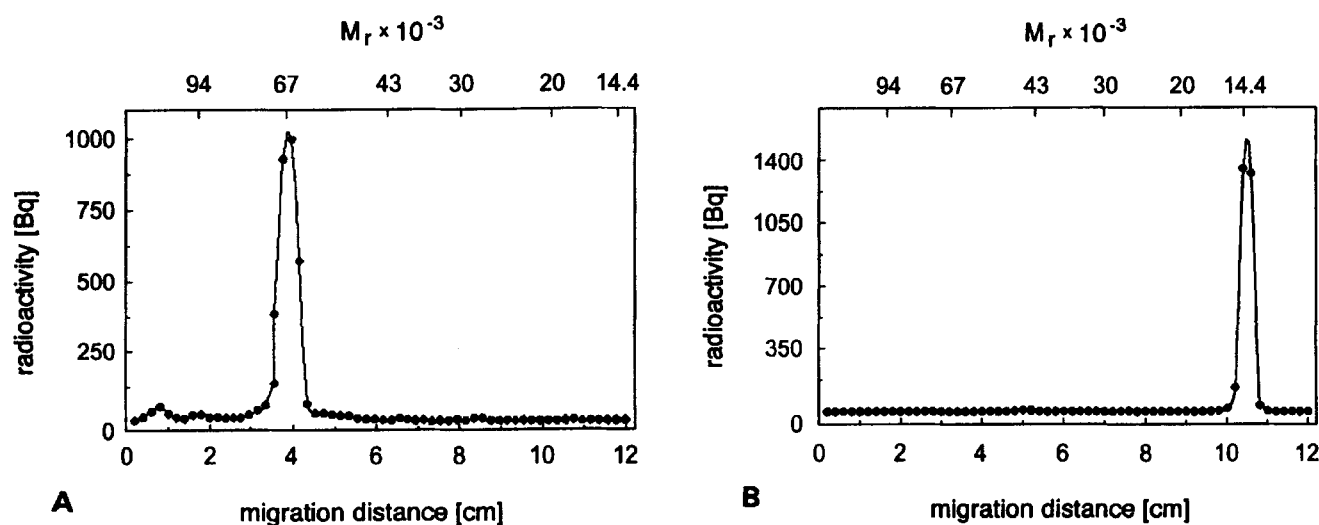
Fig. 3. Photoaffinity labeling of BSA (A) and H-FABP (B) by 11,11-azi[G-^{3}H]stearate. A solution of 1 μM of the corresponding protein in standard medium was irradiated in the presence of 30 nM (25 kBq) 11,11-azi[G-^{3}H]stearate at 350 nm and 30°C for 10 min. The samples were subjected to SDS-PAGE, and radioactivity was determined by liquid scintillation counting. A: Distribution of radioactivity of a sample of BSA after photoaffinity labeling. Total acrylamide concentration was 10.5%. B: Distribution of radioactivity of a sample of H-FABP after photoaffinity labeling. Total acrylamide concentration was 12%.
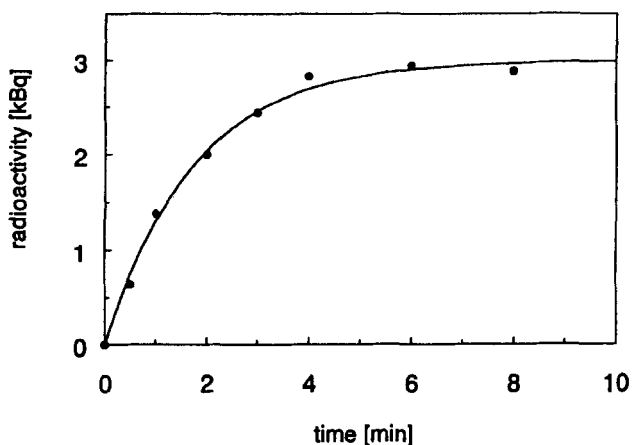
Fig. 2 Time dependency of incorporation of radioactivity during photoaffinity labeling of BAS by 11,11-azi[G-³H]stearate. Except for different irradiation times the experimental conditions were the same as in Fig. 3A.

fatty acid salt-binding proteins. This clearly indicates that the photolabile stearate derivative binds reversibly to fatty acid salt-binding proteins in the absence of irradiation. Under the experimental conditions used, photoaffinity labeling of BSA and H-FABP followed first order kinetics with half-lifes nearly identical to that of photolysis of 11,11-azistearic acid in chloroform.

Specificity of photoaffinity labeling

For demonstration of the relative specificity of the labeling process using 11,11-[G-³H]azistearate, photoaffinity labeling of BSA and H-FABP, respectively, was performed in the presence of various proteins not involved in lipid metabolism. Photoaffinity labeling of a protein mixture containing phosphorylase b, BSA, ovalbumin, carboanhydrase, and soybean trypsin inhibitor led to incorporation of radioactivity virtually only in BSA (**Fig. 5B**). Photoaffinity labeling of this protein mixture containing H-FABP instead of α-lactalbumin and no BSA resulted in the incorporation of radioactivity virtually only in H-FABP (Fig. 5C). The small extent of nonspecific labeling is demonstrated by photolyzing 11,11-azi[G-³H]stearate in the presence of polypeptides not interacting with long-chain fatty acid salts (Fig. 5D). In comparison to BSA and H-FABP, each of these polypeptides was labeled only to <2%, as shown by the 20-fold enlarged scale on the right ordinate (Fig. 5D, open symbols). In order to illustrate the comparison between specific and nonspecific labeling, the incorporation of radioactivity in the polypeptides not interacting with long-chain fatty acid salts is given in the same scale as for BSA and H-FABP on the left ordinate (Fig. 5D, filled symbols). The results of photoaffinity labeling of protein mixtures with 11,11-azi[G-³H]stearate clearly demonstrate the specificity of the interaction of binding proteins for long-chain fatty acid salts with this probe.

In order to show that 11,11-azistearate and long-chain fatty acid salts bind to the same binding sites in BSA and H-FABP, photoaffinity labeling was carried out in the
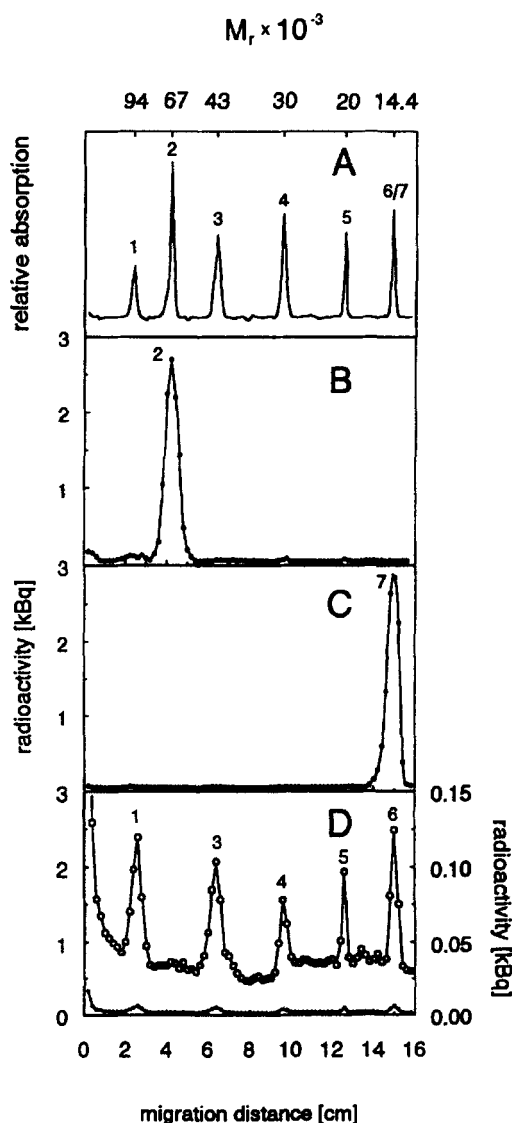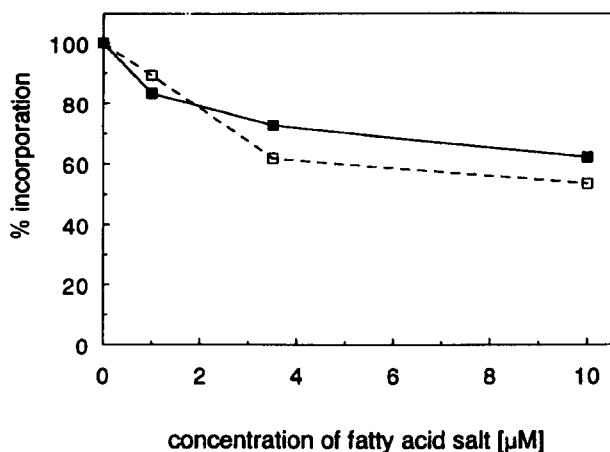

Fig. 5. Photoaffinity labeling of mixtures of purified proteins by 11,11-azi[G-³H]stearate. Mixtures of 100 μg of each protein concerned in 400 μl standard medium containing 90 nM (100 kBq) 11,11-azi[G-³H]stearate were irradiated at 350 nm and 30°C for 10 min. After SDS-PAGE using a total acrylamide concentration of 12%, radioactivity in the gel was measured by liquid scintillation counting. A: Distribution of the proteins concerned. B: Distribution of radioactivity after photoaffinity labeling of a solution containing 1, phosphorylase b (M_r 94,000); 2, BSA (M_r 67,000); 3, ovalbumin (M_r 43,000); 4, carboanhydrase (M_r 30,000); 5, soybean trypsin inhibitor (M_r 20,000); and 6, α-lactalbumin (M_r 14,400). C: Distribution of radioactivity after photoaffinity labeling of a solution containing 1, phosphorylase b; 3, ovalbumin; 4, carboanhydrase; 5, soybean trypsin inhibitor; and 7, H-FABP (M_r 14,000). D: Distribution of radioactivity after photoaffinity labeling of a solution containing 1, phosphorylase b; 3, ovalbumin; 4, carboanhydrase; 5, soybean trypsin inhibitor; and 6, α-lactalbumin. (●) Data plotted with the same scale as in B and C (left ordinate); (○) data plotted with a 20-fold enlarged scale compared to B and C (right ordinate).
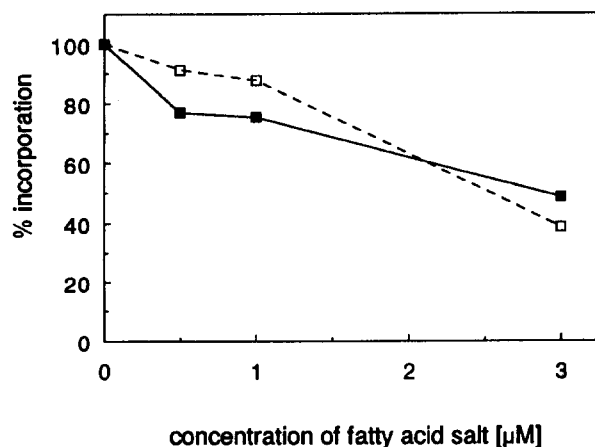
presence of different concentrations of stearate or heptafluorostearate. Whereas photoaffinity labeling is usually performed in liquid state, for studies of the competition of 11,11-azi[G-^{3}H]stearate and stearate or heptafluorostearate the irradiation procedure was performed after cryofixation in the solid deep-frozen state (36). Photoaffinity labeling in the frozen state makes use of the fact that photolytic reactions occur practically independent of temperature. In a frozen system, the complexes formed by binding protein and competing ligands are fixed at their actual state reflecting the true binding ratios. In the presence of increasing concentrations of stearate and heptafluorostearate, a clear decrease of labeling of BSA (**Fig. 6**) and of H-FABP (**Fig. 7**) was observed. Within the range of experimental variation, the same decrease of labeling of both fatty acid salt-binding proteins was obtained with stearate as well as with heptafluorostearate. These results strongly indicate that stearate, heptafluorostearate, and 11,11-azistearate bind to the same binding sites of BSA and H-FABP.

Extent of photoaffinity labeling

Photoaffinity labeling, a method usually used for the identification of binding proteins, is most selective at low concentrations of the photolabile derivative. Due to these low concentrations of the photolabile derivative, only a very small part of the binding proteins will become labeled.

Fig. 7. Photoaffinity labeling of H-FABP by 11,11-azi[G-^{3}H]stearate in the presence of stearate or heptafluorostearate. Solutions of 1 µM of H-FABP in standard medium in the presence of 30 nM (25 kBq) 11,11-azi[G-^{3}H]stearate and different concentrations of stearate or heptafluorostearate were subjected to cryofixation and subsequently irradiated at 350 nm in the deep-frozen state for 15 min. Ratios of incorporation are expressed as percentage of the values obtained in the absence of competing long-chain fatty acid salts; (■) stearate as competing fatty acid salt; (□) heptafluorostearate as competing fatty acid salt.

Photoaffinity labeling of 1 µM BSA or H-FABP using 30 nM (25 kBq) 11,11-[G-^{3}H]azistearate resulted in a maximal covalent incorporation of the applied radioactivity into both proteins of up to 10%. Under the conditions used, these yields of incorporation by a photogenerated reagent were relatively high and show that the chosen position of the diazirine function in the middle of the fatty acid salt seems to be particularly suitable for photoaffinity labeling studies. However, under these conditions only extremely small amounts of about 0.3% of the applied proteins were labeled. Where a high extent of site labeling is required, excess of concentration of the photolabile reagent over protein concentration and repeated labeling are necessary.

In order to demonstrate that the irreversible labeling of BSA and H-FABP decreased the binding capacity for long-chain fatty acid salts, photoaffinity labeling was repeated three times using a 3.3-fold molar excess of 11,11-azistearate for labeling of BSA and a 2-fold molar excess for labeling of H-FABP. During the complete experimental procedure, bivalent cations were excluded to prevent precipitation of 11,11-azistearate. Subsequent to each photoaffinity labeling, irradiation products that were not incorporated covalently were removed by Lipidex-1000 (51). Controls were performed with BSA and H-FABP in the presence of stearate instead of 11,11-azistearate and in the absence of any fatty acid salt. After the complete photoaffinity labeling procedure, binding capacities of labeled BSA and of controls were estimated for stearate and for hep-

Fig. 6. Photoaffinity labeling of BSA by 11,11-azi[G-^{3}H]stearate in the presence of stearate or heptafluorostearate. Solutions of 1 µM of BSA in standard medium in the presence of 30 nM (25 kBq) 11,11-azi[G-^{3}H]stearate and different concentrations of stearate or heptafluorostearate were subjected to cryofixation and subsequently irradiated at 350 nm in the deep-frozen state for 15 min. Ratios of incorporation are expressed as percentage of the values obtained in the absence of competing long-chain fatty acid salts; (■) stearate as competing fatty acid salt; (□) heptafluorostearate as competing fatty acid salt.

tafluorostearate, using the fluorescent probe ADIFAB as indicator for free fatty acid salt (37). The dissociation constants of ADIFAB for stearate and heptafluorostearate in standard medium without bivalent cations were determined to be 0.33 μM and 0.21 μM, respectively. Using these dissociation constants, the concentrations of free fatty acid salts in the presence of BSA were estimated from the ratios of fluorescence intensities of the free and the occupied form of ADIFAB measured at 432 nm and 505 nm, respectively. The amount of fatty acid salt bound to BSA was calculated from the total concentration less the concentration of free fatty acid salt and corrected for the portion of fatty acid salt bound to ADIFAB. The analysis revealed that about 20–30% of the binding sites of BSA were blocked irreversibly for the binding of stearate and heptafluorostearate by photoaffinity labeling under the conditions used. For H-FABP the total binding capacity after the photoaffinity labeling procedure was likewise decreased by about 20–30% for both stearate and heptafluorostearate.

Irreversible inhibition of uptake of long-chain fatty acid salts by photoaffinity labeling

In order to obtain an extent of labeling adequate for unambiguous proof of irreversible inhibition of a catalytic function, saturating conditions are required. Because the extent of saturation of a transport system parallels the rate of uptake of a substrate, a relative high uptake velocity of 11,11-azistearate must be sought. For salts of long-chain fatty acids it is well known that the rate of uptake into hepatocytes is drastically increased if BSA is added to overcome the problems caused by their extreme low solubility in aqueous solutions. Therefore, photoaffinity labeling of isolated hepatocytes by 11,11-azistearate was performed in the presence of BSA. A BSA concentration of 100 μM and a 3-fold molar excess of 11,11-azistearate proved to be favorable for irreversible inhibition of uptake of long-chain fatty acid salts. These experimental conditions ensured, on the one hand, dissolution of 11,11-azistearate at 37°C within 30 min, which is required by the restricted stability of the photolabile compound, and, on the other hand, a high rate of uptake which is necessary for a sufficient saturation of possible carrier proteins. In order to avoid dilution of the photolabile compound, the hepatocytes were centrifuged and resuspended in the incubation medium already containing 11,11-azistearate and BSA. To minimize the accumulation of photolabile compound in the interior of the cells and to exclude intracellular trapping reactions as far as possible, irradiation was started immediately after suspending the hepatocytes in the incubation medium.

Uptakes of all compounds into isolated hepatocytes were followed for the first min and proved to be linear under the conditions used for at least 40 sec, as shown for stearate (**Fig. 8**) and heptafluorostearate (**Fig. 9**). In order to examine whether the irradiation procedure used for photoaffinity labeling had an effect on uptake rates, hepatocytes were incubated and irradiated in the presence of stearate instead of its 11,11-azi derivative under otherwise identical conditions. For all compounds the rates of uptake remained unchanged by this irradiation procedure, as shown in Fig. 8 for stearate and in Fig. 9 for heptafluorostearate. Incubation of the cells with 11,11-azistearate without irradiation but performing all other experimental steps likewise did not alter the rates of uptake. In all controls the rates of uptake did not differ significantly ($P > 0.5$ for each case). This behavior of isolated intact hepatocytes towards irradiation has also been observed in the study of bile salt transport (35, 52).

Photoaffinity labeling of isolated hepatocytes with 11,11-azistearate resulted in a clear decrease of initial uptake rates of both, stearate (Fig. 8) and heptafluorostearate (Fig. 9). The rates of uptake of both compounds are diminished significantly ($P < 0.001$ for each) from 0.34 ± 0.02 to 0.23 ± 0.03 nmol/(min · mg protein) for stearate and from 0.44 ± 0.02 to 0.32 ± 0.05 nmol/(min · mg protein) for heptafluorostearate, respectively.
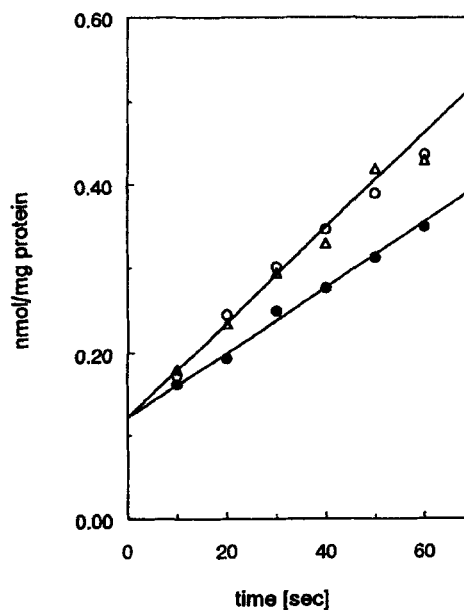

Fig. 8. Inhibition of uptake of stearate by photoaffinity labeling of hepatocytes with 11,11-azistearate. Time dependency of the uptake of 50 μM (10 kBq) [1-^{14}C]stearate in the presence of 50 μM BSA into freshly isolated hepatocytes (1×10^6–1.3×10^6 cells/ml); (○) uptake of [1-^{14}C]stearate into cells that have not been treated at all; (△) uptake of [1-^{14}C]stearate into cells that have been irradiated at 350 nm in the presence of stearate; (●) uptake of [1-^{14}C]stearate into cells that have been irradiated at 350 nm in the presence of 11,11-azistearate.

In contrast to the inhibition of uptake of long-chain fatty acid salts, photoaffinity labeling of hepatocytes with 11,11-azistearate had no significant effect on the uptake of cholyltaurine. The uptake rate of cholyl[2'-³H(N)]taurine inÝcontrol hepatocytes at a concentration of 20 μM (20 kBq) was 0.92 ± 0.11 nmol/(min · mg protein) which did not differ significantly ($P > 0.5$) from 0.91 ± 0.09 nmol/(min · mg protein). This indicates that the energy-consuming bile salt uptake is not impaired by the photoaffinity labeling procedure.

Likewise, no effect of photoaffinity labeling of isolated hepatocytes with 11,11-azistearate was observed for the uptake of 0.5 μM (37 kBq) 5β-[7β-³H]cholestane-3α,7α,12α-triol, a compound that is taken up into rat hepatocytes exclusively by passive diffusion (53). The permeability coefficient of the uptake of 5β-cholestane-3 α,7α,12α-triol into hepatocytes was 0.031 ± 0.008 cm/min before and 0.032 ± 0.008 cm/min after photoaffinity labeling. Though the standard deviations are relatively high, the mean values of the determined permeability coefficients before and after photoaffinity labeling correspond well with each other ($P > 0.5$). This indicates that photoaffinity labeling of isolated hepatocytes using 11,11-azistearate has no influence on the uptake of a compound entering the cells by simple diffusion.
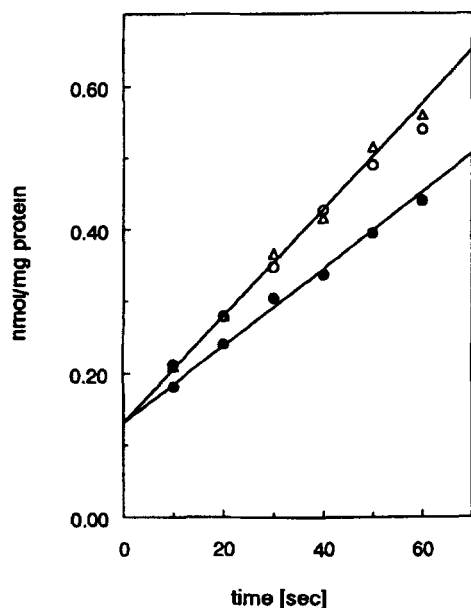

Fig. 9. Inhibition of uptake of heptafluorostearate by photoaffinity labeling of hepatocytes with 11,11-azistearate. Time dependency of the uptake of 50 μM (20 kBq) [³H]heptafluorostearate in the presence of 50 μM BSA into freshly isolated hepatocytes (1 × 10⁶–1.3 × 10⁶ cells/ml); (○) uptake of [³H]heptafluorostearate into cells that have not been treated at all; (△) uptake of [³H]heptafluorostearate into cells that have been irradiated at 350 nm in the presence of stearate; (●) uptake of [³H]heptafluorostearate into cells that have been irradiated at 350 nm in the presence of 11,11-azistearate.

In order to exclude the improbable possibility that the decreased rates of uptake of stearate and heptafluorostearate are the consequence of a lowered intracellular binding capacity, the extent of labeling of H-FABP was determined. H-FABP is the main cytosolic binding protein for salts of long-chain fatty acids after they have passed the plasma membrane of hepatocytes, as shown by photoaffinity labeling (33). Both its quantity in a given hepatocyte suspension and the extent of its photoaffinity labeling could be conveniently estimated because H-FABP is separated from other hepatic proteins by SDS-PAGE. The amount of H-FABP in freshly isolated hepatocytes was estimated at about 2% of total hepatic protein. On the basis of this value, photoaffinity labeling of isolated hepatocytes under the same conditions as used for the kinetic studies resulted in the labeling of about 2–3% of total H-FABP. Taking into consideration that about 10% of total applied 11,11-azi[G-³H]stearate were incorporated in BSA and only 1–2% in hepatic proteins, this extent of labeling is reasonable. Because only 2–3% of the total H-FABP were found to be labeled by 11,11-azistearate, the observed inhibition of uptake of long-chain fatty acid salts cannot be due to a decreased intracellular binding capacity of the hepatocytes. Thus, the decrease of the uptake rate must be caused by the irreversible inhibition of a transport system for long-chain fatty acid salts. Even if long-chain fatty acid salts have the ability to cross lipid bilayers by simple diffusion of their protonated species, a transport system in the plasma membrane of hepatocytes must exist that mediates their uptake. The molecular nature of this transport system and whether the hepatic plasma membrane fatty acid-binding protein closely related to mitochondrial glutamic-oxaloacetic transaminase (EC 2.6.1.1) (18) and/or the liver plasma membrane fatty acid-binding protein closely related or identical with mitochondrial thiolase (EC 2.3.1.9) (16, 54) are directly or indirectly involved in transport of long-chain fatty acid salts will be the aim of further studies.

Because the uptake rates of stearate and of heptafluorostearate were inhibited to nearly the same extent of about 30%, it may be concluded that both substrates share the same transport system. This, in turn, proves the suitability of heptafluorostearate as a model compound for the study of biological transport of long-chain fatty acid salts. Heptafluorostearate cannot be protonated under physiological conditions and therefore allows the study of mediated transport without being superimposed by simple diffusion (W. Schmider, A. Fahr, and G. Kurz, unpublished results). The intracellular accumulation of the metabolically inert analogue of stearate and its photolabile derivative may be useful for the identification of binding proteins

of free fatty acid salts and for the elucidation of signalling processes (55, 56). In comparison with the photolabile 11,11-azi derivative of heptafluorostearate (30), 11,11-azistearate is susceptible to metabolic transformation and should be suitable not only for the study of membrane transport of long-chain fatty acid salts but also for the identification of intracellular proteins involved in metabolism.

REFERENCES

1. Spector, A. A., D. Steinberg, and A. Tanaka. 1965. Uptake of free fatty acids by Ehrlich ascites tumor cells. *J. Biol. Chem.* **240:** 1032–1041.
2. DeGrella, R. F., and R. J. Light. 1980. Uptake and metabolism of fatty acids by dispersed adult rat heart myocytes. II. Inhibition by albumin and fatty acid homologues, and the effect of temperature and metabolic reagents. *J. Biol. Chem.* **255:** 9739–9745.
3. Westergaard, H., K. H. Holtermüller, and J. M. Dietschy. 1986. Measurement of resistance of barriers to solute transport in vivo in rat jejunum. *Am. J. Physiol.* **250:** G727–G735.
4. Noy, N., T. M. Donnelly, and D. Zakim. 1986. Physical–chemical model for the entry of water-insoluble compounds into cells. Studies of fatty acid uptake by the liver. *Biochemistry.* **25:** 2013–2021.
5. Rose, H., T. Hennecke, and H. Kammermeier. 1990. Sarcolemmal fatty acid transfer in isolated cardiomyocytes governed by albumin/membrane-lipid partition. *J. Mol. Cell. Cardiol.* **22:** 883–892.
6. Hamilton, J. A., V. N. Civelek, F. Kamps, K. Tornheim, and B. E. Corkey. 1994. Changes in internal pH caused by movement of fatty acids into and out of clonal pancreatic β-cells (HIT). *J. Biol. Chem.* **269:** 20852–20856.
7. Mahadevan, S., and F. Sauer. 1974. Effect of trypsin, phospholipases, and membrane-impermeable reagents on the uptake of palmitic acid by isolated rat liver cells. *Arch. Biochem. Biophys.* **164:** 185–193.
8. Samuel, D., S. Paris, and G. Ailhaud. 1976. Uptake and metabolism of fatty acids and analogues by cultured cardiac cells from chick embryo. *Eur. J. Biochem.* **64:** 583–595.
9. Abumrad, N. A., R. C. Perkins, J. H. Park, and C. R. Park. 1981. Mechanism of long chain fatty acid permeation in the isolated adipocyte. *J. Biol. Chem.* **256:** 9183–9191.
10. Stremmel, W., G. Strohmeyer, and P. D. Berk. 1986. Hepatocellular uptake of oleate is energy-dependent, sodium-linked, and inhibited by an antibody to a hepatocyte plasma membrane fatty acid binding protein. *Proc. Natl. Acad. Sci. USA.* **83:** 3584–3588.
11. Potter, B. J., D. Sorrentino, and P. D. Berk. 1989. Mechanisms of cellular uptake of free fatty acids. *Annu. Rev. Nutr.* **9:** 253–270.
12. Stremmel, W. 1989. Mechanism of hepatic fatty acid uptake. *J. Hepatol.* **9:** 374–382.
13. Storch, J., C. Lechene, and A. M. Kleinfeld. 1991. Direct determination of free fatty acid transport across the adipocyte plasma membrane using quantitative fluorescence microscopy. *J. Biol. Chem.* **266:** 13473–13476.
14. Harmon, C. M., P. Luce, A. H. Beth, and N. A. Abumrad. 1991. Labeling of adipocyte membranes by sulfo-N-succinimidyl derivatives of long-chain fatty acids: inhibition of fatty acid transport. *J. Membr. Biol.* **121:** 261–268.
15. Kamp, F., and J. A. Hamilton. 1993. Movement of fatty acids, fatty acid analogues, and bile acids across phospholipid bilayers. *Biochemistry.* **32:** 11074–11086.
16. Stremmel, W., G. Strohmeyer, F. Borchard, S. Kochwa, and P. D. Berk. 1985. Isolation and partial characterization of a fatty acid binding protein in rat liver plasma membranes. *Proc. Natl. Acad. Sci. USA.* **82:** 4–8.
17. Fujii, S., H. Kawaguchi, and H. Yasuda. 1987. Isolation and partial characterization of an amphiphilic 56-kDa fatty acid binding protein from rat renal basolateral membrane. *J. Biochem.* **101:** 679–684.
18. Berk, P. D., H. Wada, Y. Horio, B. J. Potter, D. Sorrentino, S-L. Zhou, L. M. Isola, D. Stump, C-L. Kiang, and S. Thung. 1990. Plasma membrane fatty acid-binding protein and mitochondrial glutamic-oxaloacetic transaminase of rat liver are related. *Proc. Natl. Acad. Sci. USA.* **87:** 3484–3488.
19. Trigatti, B. L., D. Mangroo, and G. E. Gerber. 1991. Photoaffinity labeling and fatty acid permeation in 3T3-L1 adipocytes. *J. Biol. Chem.* **266:** 22621–22625.
20. Abumrad, N. A., M. R. El-Maghrabi, E-Z. Amri, E. Lopez, and P. A. Grimaldi. 1993. Cloning of a rat adipocyte membrane protein implicated in binding or transport of long-chain fatty acids that is induced during preadipocyte differentiation. Homology with human CD36. *J. Biol. Chem.* **268:** 17665–17668.
21. Schaffer, J. E., and H. F. Lodish. 1994. Expression cloning and characterization of a novel adipocyte long chain fatty acid transport protein. *Cell.* **79:** 427–436.
22. Weisiger, R., J. Gollan, and R. Ockner. 1981. Receptor for albumin on the liver cell surface may mediate uptake of fatty acids and other albumin-bound substances. *Science.* **211:** 1048–1051.
23. Ockner, R. K., R. A. Weisiger, and J. L. Gollan. 1983. Hepatic uptake of albumin-bound substances: albumin receptor concept. *Am. J. Physiol.* **245:** G13–G18.
24. Stremmel, W., B. J. Potter, and P. D. Berk. 1983. Studies of albumin binding to rat liver plasma membranes. Implications for the albumin receptor hypothesis. *Biochim. Biophys. Acta.* **756:** 20–27.
25. Weisiger, R. A., and W-L. Ma. 1987. Uptake of oleate from albumin solutions by rat liver. Failure to detect catalysis of the dissociation of oleate from albumin by an albumin receptor. *J. Clin. Invest.* **79:** 1070–1077.
26. Trigatti, B. L., and G. E. Gerber. 1995. A direct role for serum albumin in cellular uptake of long-chain fatty acids. *Biochem. J.* **308:** 155–159.
27. Vorum, H., R. Brodersen, U. Kragh-Hansen, and A. O. Pedersen. 1992. Solubility of long-chain fatty acids in phosphate buffer at pH 7.4. *Biochim. Biophys. Acta.* **1126:** 135–142.

28. Ptak, M., M. Egret-Charlier, A. Sanson, and O. Bouloussa. 1980. A NMR study of the ionization of fatty acids, fatty amines and N-acylamino acids incorporated in phosphatidylcholine vesicles. *Biochim. Biophys. Acta.* **600:** 387–397.

29. Noy, N. 1992. The ionization behavior of retinoic acid in lipid bilayers and in membranes. *Biochim. Biophys. Acta.* **1106:** 159–164.

30. Stoll, G. H., R. Voges, W. Gerok, and G. Kurz. 1991. Synthesis of a metabolically stable modified long-chain fatty acid salt and its photolabile derivative. *J. Lipid Res.* **32:** 843–857.

31. Gengenbacher, T., W. Gerok, U. Giese, and G. Kurz. 1990. Synthesis and applicability of photolabile 7,7-azo analogues of natural bile salt precursors. *J. Lipid Res.* **31:** 315–327.

32. Kramer, W., and G. Kurz. 1983. Photolabile derivatives of bile salts. Synthesis and suitability for photoaffinity labeling. *J. Lipid Res.* **24:** 910–923.

33. Dietrich, A., W. Dieminger, K. Fuchte, G. H. Stoll, E. Schiltz, W. Gerok, and G. Kurz. 1995. Functional significance of interaction of H-FABP with sulfated and nonsulfated taurine-conjugated bile salts in rat liver. *J. Lipid Res.* **36:** 1745–1755.

34. Read, S. M., and D. H. Northcote. 1981. Minimization of variation in the response to different proteins of the Coomassie Blue G dye-binding assay for protein. *Anal. Biochem.* **116:** 53–64.

35. Schramm, U., G. Fricker, H-P. Buscher, W. Gerok, and G. Kurz. 1993. Fluorescent derivatives of bile salts. III. Uptake of 7β-NBD-NCT into isolated hepatocytes by the transport systems for cholyltaurine. *J. Lipid Res.* **34:** 741–757.

36. Falk, E., M. Müller, M. Huber, D. Keppler, and G. Kurz. 1989. Direct photoaffinity labeling of leukotriene binding sites. *Eur. J. Biochem.* **186:** 741–747.

37. Richieri, G. V., A. Anel, and A. M. Kleinfeld. 1993. Interactions of long-chain fatty acids and albumin: determination of free fatty acid levels using the fluorescent probe ADIFAB. *Biochemistry.* **32:** 7574–7580.

38. Lawson, A. M. 1989. Mass spectroscopy—the fundamental principles. *In* Mass Spectrometry. A. M. Lawson, editor. Walter de Gruyter, Berlin, New York. 1–52.

39. Still, W. C., M. Kahn, and A. Mitra. 1978. Rapid chromatographic technique for preparative separations with moderate resolution. *J. Org. Chem.* **43:** 2923–2925.

40. Hauser, C. R., B. E. Hudson, B. Abramovitch, and J. C. Shivers. 1955. *tert*-Butyl acetate. II. Acetyl chloride method. *Org. Syn. Coll.* **Vol. III:** 142–144.

41. Gundu Rao, C., S. U. Kulkarni, and H. C. Brown. 1979. Oxidation of organoboranes containing primary alkyl groups with pyridinium chlorochromate. A direct synthesis of aldehydes from terminal alkenes. *J. Organometal. Chem.* **172:** C20–C22.

42. Brown, H. C., S. U. Kulkarni, and C. Gundu Rao. 1980. Highly selective conversion of terminal olefins into aldehydes. *Syn.* **1980:** 151–153.

43. Sobotka, H., and F. E. Stynler. 1950. Neo-fatty acids. *J. Am. Chem. Soc.* **72:** 5139–5143.

44. Casteignau, G., and D. Villessot. 1968. Identification par chromatographie en phase gazeuse de composés difonctionnels insaturés. I. Synthèse et indices de rétention. *Bull. Soc. Chim. Fr.* **1968:** 3893–3903.

45. Bowers, A., T. G. Halsall, E. R. H. Jones, and A. J. Lemin. 1953. The chemistry of the triterpenes and related compounds. Part XVIII. Elucidation of the structure of polyporenic acid C. *J. Chem. Soc.* **1953:** 2548–2560.

46. Church, R. F. R., A. S. Kende, and M. J. Weiss. 1965. Diazirines. I. Some observations on the scope of the ammonia-hydroxylamine-O-sulfonic acid diaziridine synthesis. The preparation of certain steroid diaziridines and diazirines. *J. Am. Chem. Soc.* **87:** 2665–2671.

47. Church, R. F. R., and M. J. Weiss. 1970. Diazirines. II. Synthesis and properties of small functionalized diazirine molecules. Some observations on the reaction of a diaziridine with the iodine–iodide system. *J. Org. Chem.* **35:** 2465–2471.

48. Anderson, G. W., and F. M. Callahan. 1960. *t*-Butyl esters of amino acids and peptides and their use in peptide synthesis. *J. Am. Chem. Soc.* **82:** 3359–3363.

49. Stoll, G. H. 1990. Synthese metabolisch inerter Derivate langkettiger Fettsäuren und Nachweis ihrer Eignung zur Untersuchung biologischer Transport-Prozesse. 2,2,3,3,18,18,18-Heptafluorstearat und sein photolabiles Analogon. Thesis, University of Freiburg, Germany.

50. Evans, E. A. 1966. Specificity of tritium labelling. *In* Tritium and Its Compounds. Butterworth & Co., London. 263–305.

51. Glatz, J. F. C., and J. H. Veerkamp. 1983. A radiochemical procedure for the assay of fatty acid binding by proteins. *Anal. Biochem.* **132:** 89–95.

52. Dietrich, A., W. Dieminger, S. Mac Nelly, W. Gerok, and G. Kurz. 1995. Synthesis and applicability of a photolabile 7,7-azi analogue of 3-sulfated taurine-conjugated bile salts. *J. Lipid Res.* **36:** 1729–1744.

53. Wössner, R. 1994. 26,26,26,27,27,27-Hexafluor-5β-cholestan-3α,7α,12α-triol. Synthese und Eignung für Untersuchungen zum Transport und Stoffwechsel von Gallenalkoholen in Ratten und Rochen. Thesis, University of Freiburg, Germany.

54. Fitscher, B. A., E. Rodilla-Sala, T. Hashimoto, L. Ghistescu, M. Bendayan, and W. Stremmel. 1990. Molekulare Charakterisierung des fettsäurebindenden Membranproteins MFABP der Rattenleber. *Z. Gastroenterol.* **28:** 691.

55. Distel, R. J., G. S. Robinson, and B. M. Spiegelman. 1992. Fatty acid regulation of gene expression. Transcriptional and post-transcriptional mechanisms. *J. Biol. Chem.* **267:** 5937–5941.

56. Amir, E-Z., G. Ailhaud, and P-A. Grimaldi. 1994. Fatty acids as signal transducing molecules: involvement in the differentiation of preadipose to adipose cells. *J. Lipid Res.* **35:** 930–937.